International Journal of Innovative Studies in Sociology and Humanities
ISSN 2456-4931 | Open Access | Volume 7, Issue 12, 2022
DOI: https://doi.org/10.20431/2456-4931.071201

Evaluation of the Urban Expansion of the Constantine Metropolitan Area Through Landsat Remote Sensing Combined with Landscape Metrics

Adel DAIKH[1], Pr. Samira DEBACHE-BENZEGOUTA[2]

[1]*University of May 8th 1945 Guelma.*
[2]*University of Constantine 3 Salah BOUBNIDER.*

Received: November 7, 2022 **Accepted**: November 27, 2022 **Published**: December 01, 2022

Abstract

The metropolitan area of Constantine is undergoing a galloping urban expansion that is manifesting itself in significant changes in land use and occupation. The aim of this study is to analyse these changes through a diachronic approach within the limits of the current administrative division of the metropolitan area of Constantine.

To do this, we used Landsat satellite imagery (spatial scenes) over a time series of three punctuated decades (1990, 2000, 2010 and 2020) to detect the topology, rate and process of change in land use and land cover.

This approach allowed us to elaborate in a first step eight thematic maps showing unchanged and converted land use classes. These results were obtained after the acquisition and processing of "multi-spectral band raster" satellite images on the geographic information system © QGIS (V3.10.13) and more particularly its semi-automatic supervised classification process © SCP (V7.8.10) to end up with a quantification of land use and land cover change (LULC) in the form of thematic maps integrating the metadata.

The change observed is essentially characterised by a net increase in the urban area, i.e. 12,550 hectares in 2020 compared with 8,088 hectares in 1990, and therefore an increase of more than 57.55%, of which it is believed that more than half of this growth was achieved during the decade (2010-2020), which finally gives an average growth rate equivalent to 148.73 hectares per year.

However, the quantification of the modes and processes of this change is less easy to demonstrate without the use of spatial metrics, which consists of a factorial analysis of the maps obtained to obtain verifiable indices according to empirical references. The modelling of the maps for the landscape metric assessment was carried out on the © FRAGSTATS software package (V4.2).

The correlation and cross-checking of the indices resulting from the modelling enabled us to distinguish three modes of spatial aggregation of change, the first is contiguous and homogeneous to the summit conurbation (Constantine), the second is in fragmented extension of the main conurbation and its satellite towns and the last is in peri-urban extension bordering on, but fragmented in relation to, the urban limits of the conurbations constituting the macro-form of the metropolitan area.

The results of this study can be used as a decision-making aid for future urban programming or projection operations capable of formulating urbanisation schemes that are more sustainable and adaptable to the requirements of metropolitan status.

Key words: land use and land cover change, urban expansion, remote sensing, landscapes metrics, metropole of Constantine.

INTRODUCTION

Growing urbanisation is a major challenge to the sustainability of the emerging logics of Algerian metropolises. The densification of urban networks, demographic growth, social change, economic attractiveness and the appearance of new urban functions are all elements contributing to the increase in the rate of urbanisation with a massive rise in a few decades, thus accentuating the phenomenon of urban sprawl, which is essentially characterised by the overflowing of conurbations from their spatial limits (Cabrol, n.d. 2016) leading in the same way to a loss of urban centrality from the main urban centres of the metropolis to fragmented peri-urban extensions, thus generating a deferral of urbanisation(Levy 2005). Moreover, this change is driven by a random and asynchronous expansion that is often uncontrolled in the face of the urgent need for public land for housing or industrial programmes(Guérois 2006).

The objective of this study is twofold, firstly to examine this aspect of growth and the modalities that govern this expansion from a spatiotemporal perspective by quantifying and monitoring land use changes diachronically (Zhu 2017). Secondly, to characterise the process of the extension of the metropolitan structure through the reading of its urban landscape by quantifying and evaluating the indices of the landscape metrics(Aguejdad and Hubert-Moy 2016) (Herzog and Lausch, n.d.)

The main question of this study is "How to quantify and identify the change of the urban patch from Landsat satellite image metadata? Two methods are used to detect changes between different land use classes and between different landscape forms: the first by processing multi-date satellite images and the second by modelling landscape metrics.

DETECTION OF LAND COVER CHANGE FROM MULTI-DATE SATELLITE IMAGES

Metadata from satellite imagery has become an essential tool for land use planning and development due to the wide range of satellite imagery periodicity and the optimisation of spatial resolution quality. Spatial resolution and time series play an important role in identifying land surface changes (Ridd and Liu, 1998). Monitoring the evolution of the urban patch requires a fortiori prior knowledge about the factual state and temporal context of land use and land cover.

Spatial remote sensing is a process derived from geo-located satellite imagery and integrates several layers of information acquired from optical and radiometric sensors that detect the colour spectra reflected from the land cover (relief, texture and colour), so that the various reflections are compiled into one or more image bands in raster (pixelated) format.

LANDSCAPE METRICS APPLIED TO THE URBAN ENVIRONMENT

Spatial metrics, originally developed to describe landscape structures in agricultural and natural environments, have begun to attract growing interest among researchers and planners involved in the urban environment. They are applied to describe the organisation patterns of the urban and peri-urban landscape at a given date (Lehmkul and Ruggiero, 1991; Cissel et al., 1999; Fu and Chen, 2001) or to characterise the process of urban expansion (Barnsley and Barr, 1997; Alberti and Waddell, 2000; Herold et al., 2002). These metrics can be used to analyse and describe the change in the degree of spatial heterogeneity of a landscape (Dunn et al., 1991; Wu et al., 2000) and to identify the different phases and forms of urbanisation.

METHOD

Study Area

The study area is located in the North-East of Algeria (Altitude 36° 21′ north, Latitude 6° 36′ east) 389 km east of the capital Algiers and 63 km from the Mediterranean coast, the urban area is administratively constituted by the grouping of five agglomerations, a summit city (Constantine) and four other satellite cities, it is good to know that Constantine (the ancient Cirta) is an endemic city which is currently positioned as the capital of Eastern Algeria.

The urban area covers a total surface of 780.48 km² characterised by a heterogeneous landscape with important topographical variations, up to 1000 metres of altimetric differences and levels sometimes reaching 70%, to mention only the case of the historical centre of the city of Constantine (a), the latter is implanted on a rock culminating at 725 metres of altitude at the limits of a valley, this rock is melted in its middle by a canyon wide of 300 m and deep of 125 m in which flows a river "Oued Rummel" (cf. Figure 1)

The study area has an overall population of 802,300 with a density of 429.12 inhabitants/km² according to the latest general population and housing census (RGPH) of 2008.

The climate of the urban area is continental, with temperatures ranging from 25 to 40° in summer and 0 to 12° in winter, and rainfall of between 400 and 600 mm per year.

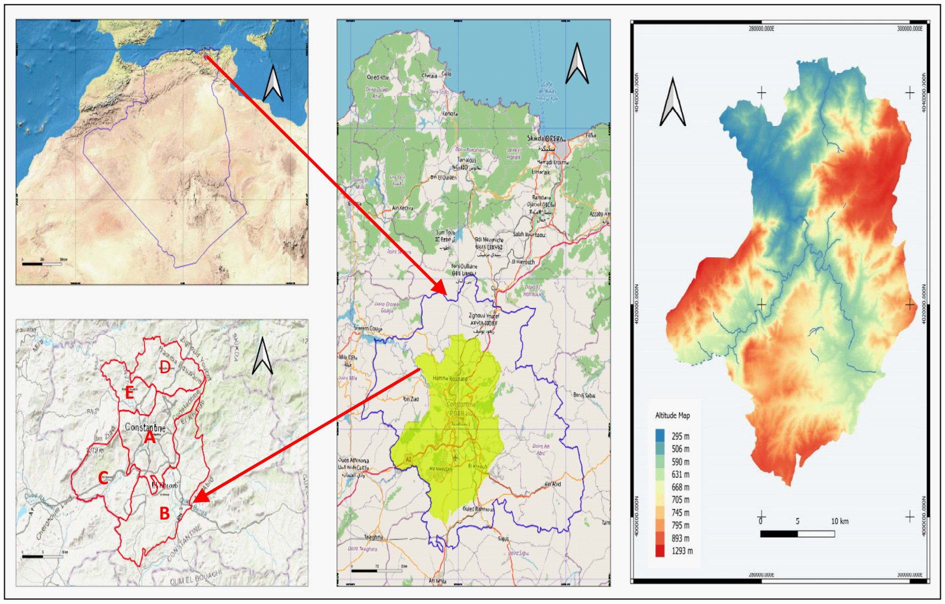

Figure 1. Location of the study area, digital elevation model DEM. (Maps made on QGIS by the authors from open Street map and Google satellite, 2022)

Materials and Data Used

The present study consists of characterising the evolution of the urban area of Constantine over a period of thirty years, i.e. between 1990 and 2020.

A period during which urban expansion seems to be more significant, for which a time series of four Landsat multi-spectral images were acquired in open access via the USGS-NASA *(United States Geological Survey) database*.

The acquired images correspond to the years: 1990, 2000, 2010 and 2020. These four satellite scenes are selected according to their temporal similarity (scenes taken during the same seasons of the year and at close times), in order to ensure better convergence in terms of atmospheric and phenological conditions *(Coppin et al., 2004; Dengsheng Lu and Weng, 2007*).

The specifications of the resulting scenes are shown in Table 1.

Table 1. Identification of the Landsat scenes used for the study*.*

Landsat_scene_ID	Sensor	Date	Bands	Cloud cover	RMSE (m)	Spatial resolution (m)
LT51940351990070FUI00	Landsat 5 TM	1990-03-11	1-2-3-4-5-7	0.0	11.196	30x30
LE71930352000115EDC00	Landsat 7 ETM+.	2000-04-24	1-2-3-4-5-7	0.0	4.583	30x30
LT51930352010198MPS01	Landsat 5 TM	2010-07-17	1-2-3-4-5-7	0.0	4.329	30x30
LC81940352020121LGN00	Landsat 8 OLI-TIRS	2020-04-30	2-3-4-5-6-7	0.0	7.196	30x30

The satellite image acquisition and processing chain is carried out using QGIS software (Congedo, 2016).

Methodological Approach

The approach followed in this study is structured in five steps: (i) pre-processing and normalization of the acquired images; (ii) a classification and post-processing (refinement) procedure; (iii) evaluation of the classification performance; (iv) post-classification comparison of the thematic maps generated after classification *(Ban and Yousif, 2016; Dengsheng Lu and Weng, 2007; Nath et al., 2014*); (v) modelling and quantification of the landscape metrics *(Aguejdad, 2016)*

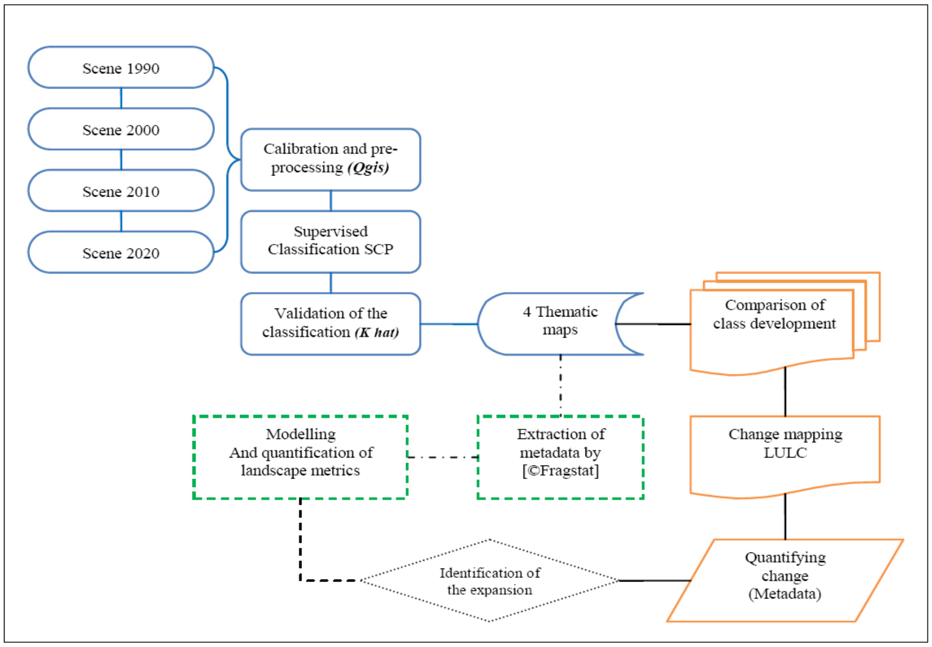

Figure 2. Flow chart of the methodological approach

Image Pre-Processing and Normalisation

The images selected for this study (L1TP level collection) are geometrically self-corrected and geocoded prior to their release by the USGS, according to the WGS 84 Zone 31 and 32 North datum. Standard RMSE (Root Mean Square Error) estimation revealed a negligible level of error (less than 0.26 pixels).

The superposition of the images is visually verified after a convergence of the four images on the same geographic system WGS 84-zone 32N, the study area is extracted through a subtraction with the vector form (shape-file) of the current administrative division accessible from the platform (DIVA-GIS). A radiometric calibration is carried out by performing a TOA (Top Of Atmospheric) correction and a subtraction of unassigned objects by applying the DOS1 (Dark Object Subtraction) model (Congedo, 2016; NASA, 2011; Tucker et al., 2004).

Following this, an enhancement of the reflectance of the images is applied to refine the quality of the images (pixel) and thus facilitate their visual reading. A false colour composition was chosen with the combination of bands (4-3-2) for the TM and ETM+ images and (5-4-3) for the (OLI-TIRS) image (Figure 3). This combination proves to be the most adequate in terms of discriminating the surfaces and objects constituting the different types of land use (Collet and Caloz, 2001; Jensen and Lulla).

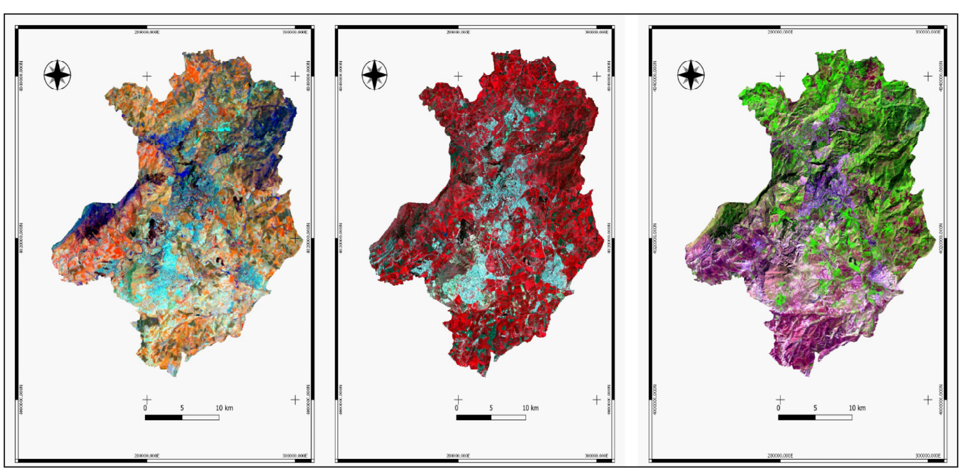

Figure 3. QGIS False colour composition of a multi-spectrum image 2000-2010-2020 Band 4-3-2 of (TM, ETM+) and 5-4-3 of (OLI-TIRS), derived by the authors from USGS

Supervised Classification and Post-Processing of Maps

The supervised classification of satellite images is an application that allows the extraction of new spatial data in addition to that already implemented on the initial scene, it consists of assigning synthetic values to a set of similar pixels, these values subsequently correspond to classes of membership in terms of land use.

Given the limitations of this study, a supervised classification was adopted (Girard and Girard, 2010; Dengsheng Lu and Weng, 2007). Taking into consideration old staff maps and based on our knowledge of the terrain, four land use classes were therefore retained for: 1-Water, 2-Vegetation (Tree and low vegetation), 3-Build-up, and 4-Bare-soil(Dechaicha, Daikh, and Alkama 2021). Each of these classes or macro-classes represents a similar group of land uses (see Table 2).

Table 2. Classification of land use by groups of similar topology

Value of the class	Label	Occupation Group/Sub-Classes
1	Water	Tributary, river, reservoir, lacquer.
2	Vegetation	Forest, tree plant, scrub, low vegetation.
3	Build-up	Residential buildings, industrial fabrics, commerce, equipment, mechanical tracks, railways.
4	Bare-soil	Bare soil, fallow land, rocky soil, agricultural soil.

These prior classifications are used to establish a macro class repository on the semi-automatic classification algorithm (SCP) (Du et al., 2014; Im and Jensen, 2005; Munafò and Congedo, 2017) by assigning numerical values to the macro classes. The sampling of the training areas (Region of interest) is established by editing the matrix image (band sets), the operation consists in manually screening the attribute polygon image for each macro class, if necessary the false colour band is modulated in adequacy with the type of class treated.

Representative areas of different classes are thus generated by the "Region Growing" algorithm, which consists in creating, from a starting pixel, a homogeneous region including pixels with similar spectral properties (Congedo, 2016; Rajendran and Mani, 2015).

The analysis of the spectral distances revealed overlaps, especially between the classes [bare soil (4) and built-up (3)].

To overcome this irregularity, we increased the number of subclasses by creating new regions of interest (ROIs) in the confusion zones by modifying the automatic thresholding settings, thus increasing the spectral separation of similar pixels. (Congedo, 2016; Sezgin and Sankur, 2004). The supervised classification is performed by the Maximum Likelihood algorithm (Dengsheng Lu and Weng, 2007; Mather and Tso, 2016; Nath et al., 2014; Phiri and Morgenroth, 2017).

The algorithm for calculating the maximum likelihood (Li) of the unknown measurement vector (x), belonging to one of the known classes (Mc), is determined on the basis of the Bayesian inference given by formula (1) :

Li (x) = ln p (ac) - [0.5 ln (|Covc|)] - [0.5(X - Mc)T(Covc - 1)(X - Mc)]...................(1)

After generation of the new classified map, a post-processing enhancement is carried out in order to correct the recalcitrant confusion areas by a manual requalification of the concerned pixels and to finish the operation by an automatic elimination of the isolated pixels by applying a 2x2 pixels filter.

This step is concluded by harmonising the four maps to obtain the same land use classes *(Dengsheng Lu and Weng, 2007)* and merging the different sub-classes into the four macro classes.

Assessment of the Veracity of the Thematic Maps by the Confusion Matrix

The verification of the classification is an essential step to ensure the veracity of the LULC maps generated before their exploitation.

It is an a posteriori test that provides information on the relevance of the classification operation, in this study we opted among others for the application of the confusion matrix since it is the most popular technique through the previous studies of *LULC & GIS.* A synthetic index derived from the confusion matrix is also used in the evaluation of accuracy. This is the Kappa coefficient (K_{hat}), which is considered a common indicator of the reliability of the classification obtained.

The principle of this test consists of an automatic randomisation on the whole map of points (1x1) pixel, these points *(Temporary Region of interest **T-ROI**)* correspond to the value of a class (x), then to ensure manually that each point corresponds to its right value on the map and in the eventuality this same point will be rectified by the attribution of the corresponding value really on the map, the number of points checked is to the benefit of obtaining good results.

The confusion matrix includes the overall accuracy ***(OA)*** and the kappa coefficient ($\boldsymbol{K_{hat}}$) as its two main evaluation indices, which are calculated by *(Kohavi and Provost)* as presented in equations (2) and (3).

For a value of (K_{hat}) greater than or equal to 0.8, the classification is considered reliable for a LULC map, if Khat varies between 0.4 and 0.8, the LULC map is considered moderately significant *(Congalton & Green, 2008; Landis & Koch, 1977).* In this study, the accuracy check was performed by generating 240 control points, randomly distributed over the study area, the confusion matrix was generated after the GIS comparison matrix was calculated.

$$\text{Overall Accuracy (OA)} = \left[\frac{(Pc) + (Nc)}{(Pc) + (Fp) + (Nc) + (Fn)} \right] X100 \ldots\ldots\ldots\ldots \ldots(2)$$

$$\text{Kappa Coefficient (K)} = \frac{OA - P(e)}{1 - P(e)} \ldots\ldots\ldots\ldots \ldots\ldots(3)$$

Detection and Calculation of Change

In this step, the thematic maps generated after the classification are subjected to a post-classification comparison operation. The aim of this analysis is to visualise and describe the process of urban expansion in the light of prior knowledge of the chronological context.When identifying the different land use changes, three time intervals are distinguished: 1990 - 2000, 2000 - 2010 and 2010-2020.

The result for each period is illustrated by a thematic map and quantified data (figure and table) corresponding to the converted and unchanged class areas. The change map shows the areas that have remained unchanged and those that have been converted during the period in question; the descriptive report illustrates quantitatively the evolution of each class by indicating the nature of the mutation (migration from one class to another).

Calculation of Landscape Metrics

Since this is an assessment of the evolution of land use and land cover classes, the landscape metrics selected for the measurement of spatio-temporal change correspond to the level of the class metrics. Six metrics were selected for this study (Herold et al., 2005; McGarigal et al., 2012): - *Number of Patches **(NP)***: calculating the number of fragments constituting a given class allows us to determine the abundance or rarity of compositional elements. Monitoring this index allows us to see whether certain fragments appear or disappear, which reveals the spatio-temporal trend (growth or decline). - Percentage of landscape ***(PLAND)***: This index refers to the percentage of area occupied by a land use class. It is an index that can indicate dominance in the composition of the landscape. - Average parcel size ***(AREA_MN):*** the average area of parcels belonging to the same class, measured in hectares (ha). The combination of this index with the (***NP)*** index allows to describe the evolution of the landscape between aggregation and/or fragmentation. For built-up areas, it reveals the mode of spatial growth (by densification or fragmentation). - *Largest Patch Index **(LPI)***: this shape index represents the portion occupied by the largest patch for a given class. The calculation of this metric indicates the level of dominance of the largest fragments of the different classes. If the LPI is close to 0, it means that the largest fragment of the class in question is minimal in the constitution of the landscape (Dechaicha, Daikh , Alkama 2021).

If ***the LPI = 100***, this fragment occupies the entire landscape. An increase in the value of this index means that the class in question tends to dominate the landscape. - *Aggregation index **(AI): This is*** a synthetic configuration index describing the organisation and arrangement of the fragments of a given land use class. The measurement of this index reveals the level of compactness (aggregation) or isolation of the fragments composing a landscape class. The value of ***(AI)*** varies between 0 and 100%. The higher the AI tends to be, the more compact the class in question tends to become and vice versa. - Normalized Landscape Shape Index ***(nLSI)***: This index corresponds to the ratio of the total number of edges ***(m)*** of the fragments to the total area of the landscape.

This index assesses the compactness of the landscape (or otherwise the disaggregation of fragments) and its geometric complexity (Dechaicha.2021)

The value of (***nLSI)*** varies between 0 and 1. (***nLS)*** which means that the landscape is perfectly compact (it has a square shape). Increasing the value of ***(nLSI)*** implies a decrease in the aggregation (or compactness) of the landscape and its shape becomes more complex, i.e. the edges become more elongated. Table 2 provides the equations for calculating these parameters and a description of their ranges. Table 2. Method of calculating the selected parameters (Neel et al., 2004; O'Neill et al., 1988). Using the thematic maps from the satellite image classification as input, the calculation of these metrics was performed using the open source software © *FRAGSTAT*.

With regard to the evaluation of the results and given the complexity of the landscapes studied, we proceeded to a correlation of these metrics in order to develop a synthetic interpretation considering the overall behaviour of the different metrics examined.

Metric	Description	Range
NP (Units)	$NP = n_i$ n_i: number of patches in the landscape of patch type (class) *i*	NP ≥ 1
PLAND (%)	$PLAND = P_i = \frac{\sum_{j=1}^{n} a_{ij}}{A}(100)$ P_i: proportion of the landscape occupied by patch type (class) *i*. a_{ij}: area (m²) of patch *ij*. A: total landscape area (m²).	0 < PLAND ≤ 100
AREA_MN (ha)	$AREA\_MN = \frac{\sum_{j=1}^{n} x_{ij}}{n_i}$ x_{ij}: total class area (m²) of patch *ij*. n_i: number of patches in the landscape of patch type (class) *i*	AREA_MN ≥ 0
LPI (%)	$LPI = \frac{\max(a_{ij})}{A}(100)$ a_{ij}: area (m²) of patch *ij*. A: total landscape area (m²).	0 < LPI ≤ 100
AI (%)	$AI = \left[\frac{g_{ii}}{max^{\rightarrow} g_{ii}}\right](100)$ g_{ii}: number of like adjacencies (joins) between pixels of patch type (class) *i*. max-g_{ii}: maximum number of like adjacencies (joins) between pixels of patch type (class) *i*.	0 ≤ AI ≤ 100
nLSI (without unit)	$nLSI = \frac{e_i - \min e_i}{\max e_i - \min e_i}$ e_i: total length of edge (or perimeter) of class *i*. min e_i: minimum total length of edge (or perimeter) of class *i*. max e_i: maximum total length of edge (or perimeter) of class *i*.	0 ≤ nLSI ≤ 1

Figure 4. Nomenclature table of landscape metrics used According to (Aguejdad and Hubert-Moy, 2016; McGarigal et al., 2012; Skupinski et al., 2009; Dechaicha and Alkama, 2020)

RESULTS AND DISCUSSION

Validation of Classification Results

The resulting thematic maps are shown in Figure 4, corresponding to the years 1990, 2000, 2010 and 2020 respectively. The confusion matrices generated for these three maps showed a satisfactory level of accuracy, both for the overall accuracy and for the accuracy of the classes, particularly those of urbanised areas and bare soil. The Kappa index ***(K_{hat})*** thus showed an acceptable level of accuracy with values of 0.78, 0.81, 0.84 and 0.89. The summary of this assessment is shown in Table 3.

Table 3. Results of the confusion matrix (map accuracy)

Type of assessment	1990	2000	2010	2020
Overall accuracy %.	86.15%	91.68%	90.23%	94.05%
User Accuracy (UA) Class 3	82.20%	89.30 %	84.66%	82.85%
User Accuracy (UA) Class 4	88.15%	94.66 %	92.33%	96.66%
User Accuracy (UA) Class 2	88.01%	91.08 %	93.70 %	84.44%
Kappa index (k_{hat})	0.78	0.81	0.84	0.89

Mapping Change: Significant Land Artificialisation

The detection of change has led to a spatiotemporal map (Figure 3) illustrating the evolution of the urban area between 1990 and 2020. At first glance, the diachronic reading of the four maps shows a clear growth of urbanised surfaces versus a significant decline in vegetated surfaces and bare soil, with the exception of the period 1990-2000, which was marked by a gain in vegetated surfaces that can be explained by a decline in exploitation (agrarian and pastoral) on the edges of the forests due to the security crisis that the country experienced, During this same period, the artificial surface area experienced a slight decline (-235 ha) between, this decline can be explained by the recovery of the land formerly occupied by precarious housing (uncontrolled urbanism) at the level of the edges of the mother city of Constantine (cf. table 4).

Table 4. Quantification of the evolution of the classes

Class	Area [Ha]				Change (+/-) Ha		
	1990	2000	2010	2020	1990-2000	2000-2010	2010-2020
Water	58	57	33	63	-1	-24	+30
Vegetation	7727	11079	3830	3280	+3352	-7249	-550
Build-up	8088	7843	8514	12550	-245	+671	+4036
Bare-soil	62019	59059	65623	62155	-2960	+6564	-3468

Overall, the expansion of the urban area has been mainly in four directions (south, south-east), particularly between 2000-2020 and (north, north-west) between 1990-2010 (see figure 5).

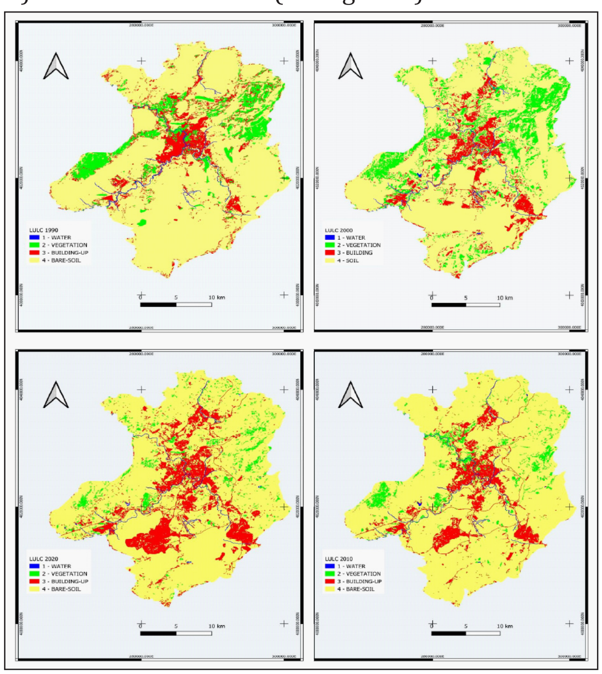

Figure 5. QGIS map with land use and land cover classes between (1990 -2020), source: authors

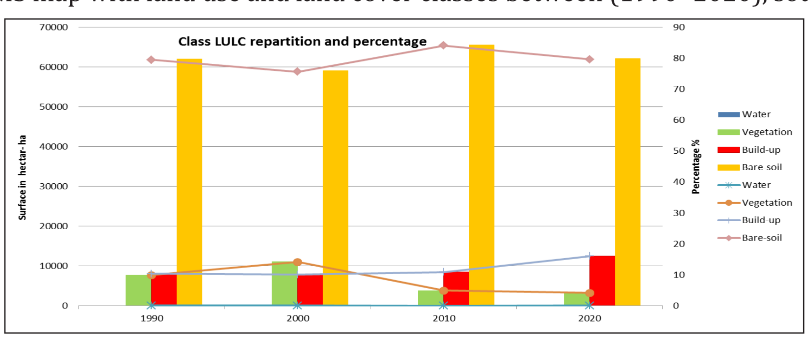

Graph 1. Land use rates and areas per year between (1990 -2020)

The first period, 1990-2000, was characterised by a weak and discontinuous urban expansion in relation to the mother city, which took place in two ways: an uncontrolled way in the form of new illegal districts, which is manifested by the conversion of vegetated land, as in the case of the "Benchergui (A)" district located at the foothills of the "Chetaba (A)" forest (north-east of Constantine), and of the "Mazia" district located on the southern hills of Constantine (cf. figure 5)

A second voluntary mode, in the form of a hybrid urban unit (collective and individual housing) as is the case of the "Ain el Bey (A)" plateau in the south of the metropolitan area and "Djebel el-Ouahch (A)" in the north. It should also be pointed out that the satellite towns are not left out of this postulate, as they have undergone spatial transformations by overflowing their original nuclei, as in the case of Khroub (a), Ain Smara (c) and Didouche Mourad (d), or by a scattered and contiguous extension in relation to the town centre, as in the case of Hamma Bouziane

The second period 2000-2010 is marked by a significant change in land use and occupation, notably with the appearance of urban sprawl driven largely by large-scale urban operations, as in the case of the new towns of Ali-Mendjeli and Massinissa (B). This period is marked by a clear decline in vegetated areas compared to the first period, a decline caused by the resumption of pastoral and agrarian activities, but also to a large extent by repeated forest fires. The third period 2010-2020 is marked by a net rise in peri-urban growth +4036 hectares, a growth that has taken place in contrast to the occupations of bare and vegetated land, which have fallen by -3468 and -550 hectares respectively.

To better understand the evolution and rate of change of land use between 1990-2020, the results are illustrated in graphs 1, 2 and 3.

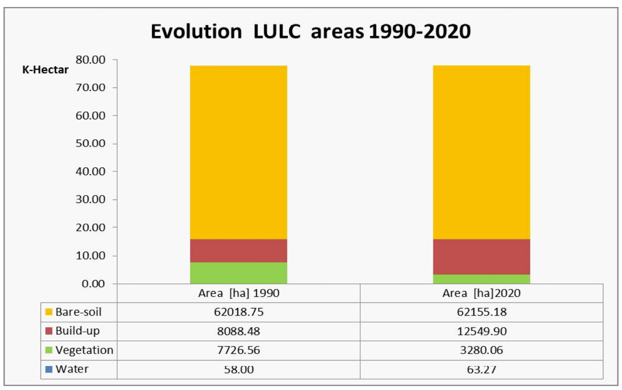

Graph 2. Area distribution of land use change between (1990 - 2020).

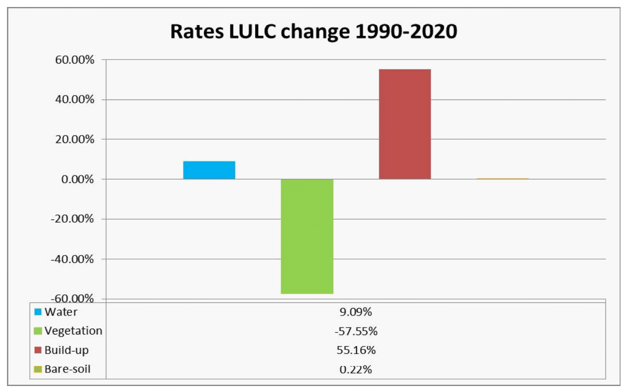

Graph 3. Rate of land use change between (1990 - 2020)

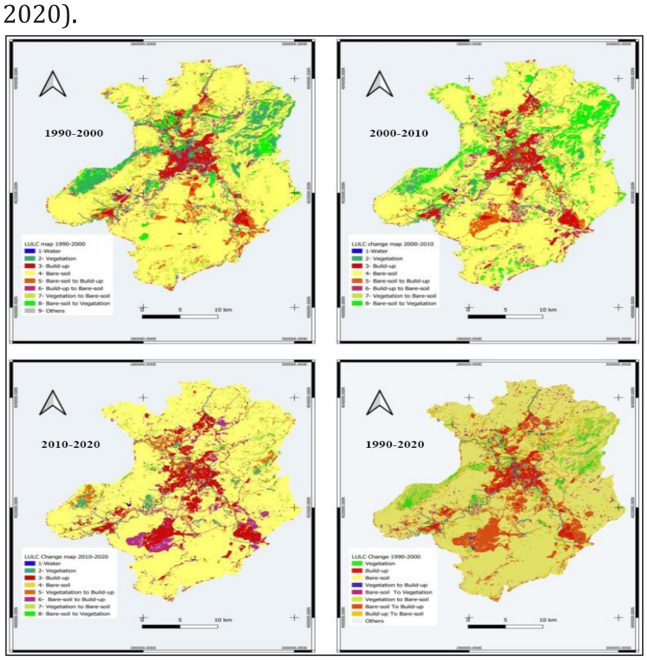

Figure 6. QGIS mapping of land use class change, source: authors

The detection of land use change shows several types of spatial conversion, but the most striking fact is that the vegetated areas have been eroded, giving way to bare land which has in turn been converted into urbanised land, so that the share of bare land remains unchanged at the expense of a considerable decrease in vegetation cover (cf. Figure 6).

Quantifying Landscape Metrics; Understanding Aggregations of Spatial Change

The urban framework of the Constantine metropolis is based on the alternation of town and country around its urban core. Four main components form the basis of this urbanisation model known as the 'metropolitan archipelago' (AUDIAR, 2004): (1) the agglomerated city-centre or central metropolitan core; (2) a framework of satellite towns on the immediate periphery of the agglomerated central core; (3) a ring of peri-urban fringe on the immediate periphery of the centre; (4) a road and rail network arranged in a star shape and playing a role in structuring the territory.

According to Allain (2004), this macro-form of urban expansion (Archipelago), which he describes as a discontinuous polycentric model with medium-sized peripheral polarities. In Table 5, the values of the landscape metrics obtained from the FRAGSTAT modelling are shown, in relation with class 2 (Build-Up).

Table 5. Quantification of landscape metrics, (Class Build-Up)

Year	PLAND	NP (Units)	LPI %.	AREA_MN (Ha)	ENN_MN (m)	LSI %.	AI %.
1990	10.37	1611	3.46	5.0209	127.6421	69.44	82.66
2000	10.05	780	3.21	10.0558	166.5355	52.04	94.33
2010	10.92	549	4.98	15.5094	215.2657	46.63	81.21
2020	16.08	840	10.77	14.9407	178.7197	50.03	96.76
Gross evolution 1990-2020	+5.71	-771	+7.31	+9.92	+51.07	-19.41	+14.10

Evolution of Surface Indicators (NP, LPI & PLAND)

The results of the surface metric calculations are shown in the following figure:

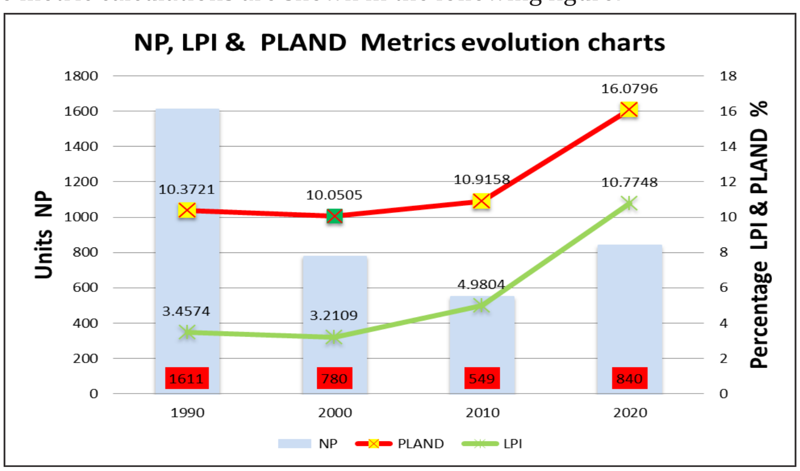

Graph 4. Evolution of landscape area metrics (1990 - 2020)

At the outset, we note that between 1990 and 2020, the number of urban fragments (UFs) fell by -47%, with a decrease of (-771) fragments (see Table 5).

However, the downward trend in this metric is discontinuous and shows two distinct periods (see graph 4). The decrease in the number of fragments is marked over the period 1990-2010 and especially, between (1990-2000), while a moderate increase is observed over the period (2010-2020). This metric highlights a process of diffusion according to which the urban expansion observed between 1990 and 2000 took place without the creation of new fragments far from the already existing urban area, especially at the level of the satellite towns where the expansion took place in a contiguous manner and in coalescence with the old urban fabric. From 2010 onwards, the results indicate a slight increase in the number of urban fragments. This second phase marks the beginning of a change in the spatial structuring of the urban patch, in which a diffuse creation of newly urbanised surfaces is taking place.

At the same time, this decrease in fragmentation has been accompanied by a continuous increase in the portion of the PLAND urban patch passing from 10.37% to 16.08% and in the index of the largest fragment LPI, which rose from 3.46% in 1990 to 10.77% in 2000 (see graph 4). The results of these area-based indicators converge with the results obtained previously from the detection of land use change.

Evolution of Distance Indicators (ENN_MN & AREA_MN)

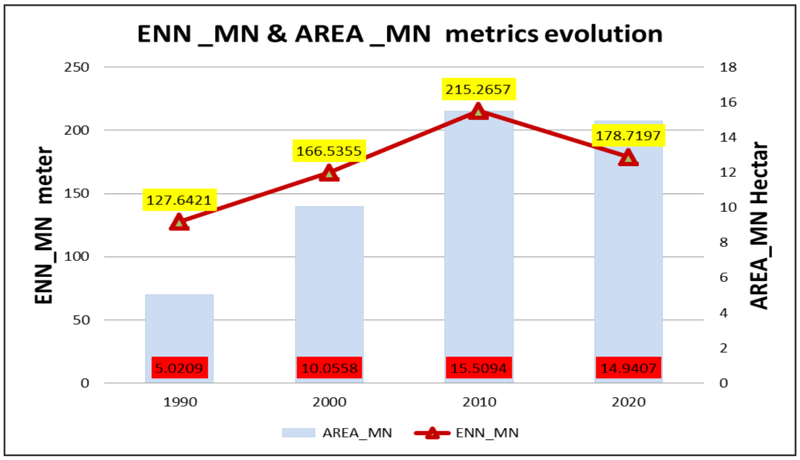

Graph 5. Evolution of landscape distance metrics (1990-2020)

This figure shows that the built-up area class has recorded a two-fold evolution in terms of the average size of the urban patch (fragment) AREA-MN and the average distance between fragments (ENN_MN), which reached their peaks between 1990-2010 with respective values of (15.5 ha) and (215.26 m), followed by a slight recession between 2010-2020 (cf. graph5) .

These results show a decrease in connectivity between the components of the urban patch accompanied by a decrease in fragmentation between (1990-2010) when the evolution of the built-up area was oriented towards a single direction and with a sustained rhythm, the distance between fragments increases as the number of fragments increases. This is explained in situ by a discontinuous and unidirectional urban expansion in opposition to the central urban core (case of the new town), The second downward trend between 2010 and 2020 shows a rebalancing of connectivity due to the appearance of new urban patches in other directions and closer to the central core, which increases connectivity, but on the other hand slightly increases the fragmentation of the urban patch (case of the urban poles, Ain Nehass and Didouche).

Evolution of the Configuration Indicators (AI and LSI)

The two histograms below illustrate the values of the spatial morphology indices (fragment compactness and fragment edge elongation).

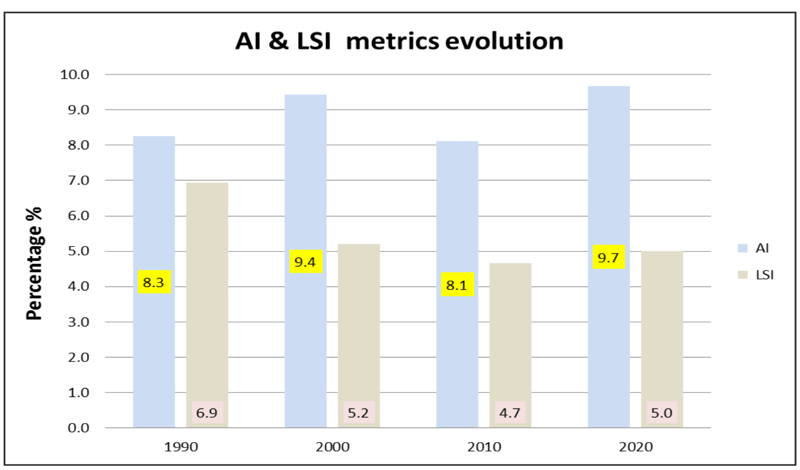

Graph 6. Evolution of landscape configuration metrics (1990-2020)

The saw tooth evolution of the value (AI) is not really significant (8.3% to 9.7%) which corresponds globally to a macro form which remains non-compact notwithstanding the important rate of urban growth demonstrated previously, it means that the extensions were operated in distance with respect to the central core, nevertheless the rise of this index between (1990-2000) demonstrates the existence of a spatial aggregation in contiguous extension with respect to the central core, The second segment of the "Shed" is linked to the process of the creation of new cities (Ali-Mendjeli and Massinissa) and their growths, therefore the redundancy of this variation can be interpreted as a fragmented macro form which tends towards a bi-cephalism.

The index (LSI) initially shows a low rate and a downward trend from (6.9% to 5.0%), this demonstrates a simple geometric composition of the urban fragments, this result corroborates the maps which illustrate urban edges with a non-elongated shape, thus an urban front with a regular geometry.

DISCUSSION

The results obtained are conclusive, they illustrate perfectly a clear progression of the urban fabric, which is particularly intense in the South, is unevenly distributed in space but with different decennial growth rates.

In the light of the results obtained from the diachronic reading, we can deduce that the metropolitan structure of Constantine is evolving towards a fragmented polycentric typology, a model that is characterised by a fairly classic configuration for polycentric metropolitan areas, where one centrality dominates the others numerically. It may be the result of the two cases of incorporation of secondary cities and centrifugal growth mentioned by Champion (2001). (Le Néchet 2015).

The low resolution Landsat satellite images (30x30m) offer significant information at a local scale (urban spot, metropolis) thanks to the large swath (185x185)km, however they remain limited when it comes to smaller scales such as urban developments and neighbourhoods, this last postulate explains the non-significant results of the configuration indicators.

CONCLUSION

The evaluation of the urban expansion of the metropolitan area of Constantine through the use of remote sensing and landscape metrics allowed us to detect and monitor the change through the quantification of land use and the quantification of landscape metrics inherent to this change over a period of three decades.

It emerges from this diachronic reading of the maps and the figures obtained that the metropolis of Constantine has undergone significant urban sprawl. The cartography obtained has enabled us to identify the typology of conversions that have occurred on the land use, and we have therefore concluded that the increase in the urban area has been made indirectly (without direct intervention) to the detriment of the vegetated surface, which has undergone a decline of the order of (-57%), The striking fact is that the change in bare soil has reached parity values during the period (1990-2020) because of its conversion which has been done in two directions, either in depreciation towards the urban area or in compensation from the vegetated area. This suggests that the metropolitan area is comparable to a macro system whose weak link is probably the green grid.

Moreover, one of the potential uses of the landscape metric in a territorial prospective approach is the evaluation of the impact of different land use scenarios on the modification of the metropolitan structure.

The results obtained can also be used to retain empirical models for predicting land use and land cover changes.

Remote sensing and monitoring of change through GIS combined with landscape metrics are among others a tool of choice for strategic planning, which will allow the developer to achieve urban operations with the least negative impact on the environment by controlling urban sprawl and non-rational land consumption, thus limiting the segregation of spaces and exploiting more other potentialities.

REFERENCES

1. Aguejdad, Rahim, et Laurence Hubert-Moy. « Suivi de l'artificialisation du territoire en milieu urbain par télédétection et à l'aide de métriques paysagères. Application à une agglomération de taille moyenne, Rennes Métropole ». Cybergeo: European Journal of Geography, 25 janvier 2016. https://doi.org/10.4000/cybergeo.27465.

2. Alqahtany, Ali. « GIS-Based Assessment of Land Use for Predicting Increase in Settlements in Al Ahsa Metropolitan Area, Saudi Arabia for the Year 2032 ». Alexandria Engineering Journal 62 (2023). https://doi.org/10.1016/j.aej.2022.07.020.
3. Al-Shaar, Walid, Jocelyne Adjizian Gérard, Nabil Nehme, Hassan Lakiss, et Liliane Buccianti Barakat. « Application of Modified Cellular Automata Markov Chain Model: Forecasting Land Use Pattern in Lebanon ». Modeling Earth Systems and Environment 7, no 2 (juin 2021): 1321 35. https://doi.org/10.1007/s40808-020-00971-y.
4. Assoul DECHAICHA. « La soutenabilité de la ville au Sahara entre compacité et tendances d'étalement urbain. Cas d'étude : Les grandes villes du Bas-Sahara algérien ». Biskra, 2020.
5. Benlakhlef, Brahim. « L'aire métropolitaine, un nouveau champ d'analyse de la ville algérienne. L'exemple d'Annaba. », 25 octobre 2008.
6. Cabrol, Yann. « Le fait urbain, un atout pour la construction métropolitaine », 2016, 2.
7. Dechaicha, Assoule, et Djamel Alkama. « Suivi et quantification de l'urbanisation incontrôlée: une approche basée sur l'analyse multitemporelle des images satellitaires LANDSAT. Cas de la ville de Bou-Saada (Algérie) ». Revue Française de Photogrammétrie et de Télédétection 223 (3 décembre 2021): 159 72. https://doi.org/10.52638/rfpt.2021.595.
8. Dechaicha, Assoule, et Adel Daikh. « Monitoring and Landscape Quantification of Uncontrolled Urbanisation in Oasis Regions: The Case of Adrar City in Algeria ». Journal of Contemporary Urban Affairs (JCUA) 5 (12 août 2021): 209 19. https://doi.org/10.25034/ijcua.2021.v5n2-5.
9. Dechaicha, Assoule, et Alkama Djamel. « LA DÉTECTION DU CHANGEMENT DE L'ÉTALEMENT URBAIN AU BAS-SAHARA ALGÉRIEN : APPORT DE LA TÉLÉDÉTECTION SPATIALE ET DES SIG. CAS DE LA VILLE DE BISKRA (ALGÉRIE) ». Revue Française de Psychanalyse 222 (12 mars 2021): 43 51.
10. Entretiens du CERTU, et Jean-Claude Gallety, éd. Renouveler les approches des phénomènes urbains. Lyon: CERTU, 2013.
11. Fusco, Giovanni. « La revanche de la forme urbaine. » In URBAN FEEDBACK Perspectives critiques sur 50 années d'enseignement et de recherche en urbanisme (1968-2018). Grenoble, France, 2020. https://hal.archives-ouvertes.fr/hal-03533125.
12. Guerni, Hassina. « Aire métropolitaine: approche dynamique de l'organisation spatiale (cas de Constantine). », s. d., 13.
13. Guérois, Marianne. « Les formes des villes européennes vues du ciel. Une contribution de l'image CORINE Land cover à la comparaison morphologique des grandes villes d'europe occidentale ». In Quatre ans de recherche urbaine 2001-2004. Volume I, édité par Émilie Bajolet, Marie-Flore Mattéi, et Jean-Marc Rennes, 121 26. Presses universitaires François-Rabelais, 2006. https://doi.org/10.4000/books.pufr.1121.
14. Guérois, Marianne, Antonin Pavard, Anne Bretagnolle, et Hélène Mathian. « Les temps de transport pour délimiter des aires urbaines fonctionnelles ? » Belgeo. Revue belge de géographie, no 2 (30 juin 2016). https://doi.org/10.4000/belgeo.17789.
15. Herzog, F, et A Lausch. « Supplementing Land-Use Statistics with Landscape Metrics: Some Methodological Considerations », s. d., 14.
16. Kamaraj, Manikandan, et Sathyanathan Rangarajan. « Predicting the Future Land Use and Land Cover Changes for Bhavani Basin, Tamil Nadu, India, Using QGIS MOLUSCE Plugin ». Environmental Science and Pollution Research, 3 février 2022. https://doi.org/10.1007/s11356-021-17904-6.
17. Koko, Auwalu Faisal, Wu Yue, Ghali Abdullahi Abubakar, Roknisadeh Hamed, et Akram Ahmed Noman Alabsi. « Monitoring and Predicting Spatio-Temporal Land Use/Land Cover Changes in Zaria City, Nigeria, through an Integrated Cellular Automata and Markov Chain Model (CA-Markov) ». Sustainability 12, no 24 (2020): 10452. https://doi.org/10.3390/su122410452.

18. Lajoie, Gilles. « Chapitre I : Le traitement des données par carroyage ». In Le Carroyage des informations urbaines : Une nouvelle forme de banque de données sur l'environnement du Grand Rouen, 5 62. Nouvelles donnes en géographie. Mont-Saint-Aignan: Presses universitaires de Rouen et du Havre, 2018. http://books.openedition.org/purh/8184.
19. BelvedeЯ +. « Le fait urbain, un atout pour la construction métropolitaine », 6 décembre 2016. https://www.revue-belveder.org/index.php/le-fait-urbain-un-atout-pour-la-construction-metropolitaine/.
20. Le Néchet, Florent. « De la forme urbaine à la structure métropolitaine : une typologie de la configuration interne des densités pour les principales métropoles européennes de l'Audit Urbain ». Cybergeo: European Journal of Geography, 18 février 2015. https://doi.org/10.4000/cybergeo.26753.
21. Levy, Albert. « Formes urbaines et significations : revisiter la morphologie urbaine ». Espaces et sociétés 122, no 3 (2005): 25 48. https://doi.org/10.3917/esp.122.0025.
22. Losiri, Chudech, et Masahiko Nagai. « Identification of Urban Expansion Patterns in Bangkok Metropolitan Region Through Time Series of Landsat Images and Landscape Metrics ». In Geoinformatics for Sustainable Development in Asian Cities, édité par Sathaporn Monprapussorn, Zhaohui Lin, Asamaporn Sitthi, et Parichat Wetchayont, 32 45. Springer Geography. Cham: Springer International Publishing, 2020. https://doi.org/10.1007/978-3-030-33900-5_4.
23. Luca Congedo. « Semi-Automatic Classification Plugin Documentation. » Journal of Open Source Software, s. d.
24. Réseau MAPS. « Modèle Christaller ». Consulté le 21 août 2022. https://maps.hypotheses.org/production-pedagogique-de-maps/modeles-mapsiens/modele-christaller.
25. MohanRajan, Sam Navin, Agilandeeswari Loganathan, et Prabukumar Manoharan. « Survey on Land Use/Land Cover (LU/LC) Change Analysis in Remote Sensing and GIS Environment: Techniques and Challenges ». Environmental Science and Pollution Research 27, no 24 (août 2020): 29900 926. https://doi.org/10.1007/s11356-020-09091-7.
26. Oliveira, Alex. « Analyse morphologique : des systèmes urbains à l'architecture de la ville », s. d., 70.
27. Rana, Md. Sohel, et Subrota Sarkar. « Prediction of Urban Expansion by Using Land Cover Change Detection Approach ». Heliyon 7, no 11 (novembre 2021): e08437. https://doi.org/10.1016/j.heliyon.2021.e08437.
28. « Région urbaine - Qu'est-ce que c'est, définition et concept - 2021 - Économie-Wiki.com ». Consulté le 21 août 2022. https://economy-pedia.com/11033051-urban-region.
29. Singh, Bhavna, Veluswamy Venkatramanan, et Benidhar Deshmukh. « Monitoring of land use land cover dynamics and prediction of urban growth using Land Change Modeler in Delhi and its environs, India ». Environmental Science and Pollution Research, s. d., 1 21. https://doi.org/10.1007/s11356-022-20900-z.
30. Skupinski, Grzegorz, Dong BinhTran, et Christiane Weber. « Les images satellites Spot multi-dates et la métrique spatiale dans l'étude du changement urbain et suburbain – Le cas de la basse vallée de la Bruche (Bas-Rhin, France) ». Cybergeo : European Journal of Geography, 12 mars 2009. https://doi.org/10.4000/cybergeo.21995.
31. Smigra, Rue Abdellah. « Antenne Régionale – Annaba – », s. d., 70.
32. Zhu, Zhe. « Change Detection Using Landsat Time Series: A Review of Frequencies, Preprocessing, Algorithms, and Applications ». ISPRS Journal of Photogrammetry and Remote Sensing 130 (1 août 2017): 370 84. https://doi.org/10.1016/j.isprsjprs.2017.06.013.

Citation: **Adel DAIKH, Pr. Samira DEBACHE-BENZEGOUTA***. Evaluation of the Urban Expansion of the Constantine Metropolitan Area Through Landsat Remote Sensing Combined with Landscape Metrics. Int J Innov Stud Sociol Humanities. 2022;7(12): 01-14. DOI: https://doi.org/10.20431/2456-4931.071201.*